

# Confounding-Robust Policy Improvement with Human-AI Teams

Ruijiang Gao,<sup>1</sup> Mingzhang Yin<sup>2</sup>

<sup>1</sup>University of Texas at Austin, <sup>2</sup>University of Florida

## Abstract

Human-AI collaboration has the potential to transform various domains by leveraging the complementary strengths of human experts and Artificial Intelligence (AI) systems. However, unobserved confounding can undermine the effectiveness of this collaboration, leading to biased and unreliable outcomes. In this paper, we propose a novel solution to address unobserved confounding in human-AI collaboration by employing the marginal sensitivity model (MSM). Our approach combines domain expertise with AI-driven statistical modeling to account for potential confounders that may otherwise remain hidden. We present a deferral collaboration framework for incorporating the MSM into policy learning from observational data, enabling the system to control for the influence of unobserved confounding factors. In addition, we propose a personalized deferral collaboration system to leverage the diverse expertise of different human decision-makers. By adjusting for potential biases, our proposed solution enhances the robustness and reliability of collaborative outcomes. The empirical and theoretical analyses demonstrate the efficacy of our approach in mitigating unobserved confounding and improving the overall performance of human-AI collaborations.

## 1 Introduction

In recent years, policy learning has emerged as a powerful tool for learning and optimizing decision-making policies across a diverse range of applications, including healthcare, finance, and marketing. One of the most promising avenues for leveraging machine learning is policy learning on observational data [1], which aims to infer optimal decision rules from historical data without the need for costly randomized experiments. Observational data, generated from real-world systems, is abundant and easily accessible, making it an attractive source for training models that can guide policy decisions.

Many algorithms have been proposed for efficient policy learning from observational data [2, 3, 4, 5], usually under the disputable *unconfoundness* assumption. It assumes there are

no hidden confounders that simultaneously influence both the treatment assignment and individual outcomes [6]. This assumption is defensible in certain domains such as automated recommendation [7] or pricing systems [8] where we have full control of the historical algorithm, but may never hold true for domains where the observational data is generated by human decision-makers.

Consider a healthcare scenario, where observational data is generated by human experts in the form of electronic health records (EHRs). These records contain a wealth of information about patients’ medical histories, treatments, and outcomes, which can be used to inform policy learning for personalized medical interventions. However, human experts, such as physicians, may seek additional information when making decisions about patient care, such as the patient’s lifestyle, mental well-being, or other contextual factors such as bedside information that might influence their decision-making process. This additional information, although crucial for decision-making, may not be systematically recorded in the EHRs, leading to potential confounding issues in the observational data. In this case, the unobserved confounding factors can result in biased estimates of optimal actions and reduce the reliability of learned policies. For example, if a physician prescribes a certain medication to patients with a specific lifestyle that is not recorded in the EHRs, the observed treatment might be confounded by the unmeasured lifestyle factor. To address the confounding problem, [5, 9] propose to use the marginal sensitivity model (MSM) to bound the possible value of the true propensity score by the degree of potential confounding in the historical data. In doing so, policy learning is formulated as a constraint optimization problem, which can be efficiently solved using observational data together with a specified confounding strength factor.

In this paper, we propose a human-AI collaboration system to improve a purely algorithmic approach by incorporating human evaluations. Certain tasks in the proposed human-AI system are executed by human experts while others are handled by the algorithm. Considering that the historical data in our motivating example are all generated by human decision-makers, an AI-only algorithm is likely to be inferior to humans in cases where external information, such as patients’ lifestyles, is necessary for optimal decision-making. The benefit of human involvement stands out in the confounding setting as human decision-makers are adept at making choices based on (unobserved) confounding factors [10]. We refer to this problem as *deferral collaboration under unobserved confounding* [11].

By adopting a human-AI collaborative approach, we can alleviate the impact of these unobserved confounders in the usual deferral collaboration. In addition, human experts can provide the AI system with insights about the additional information they consider during decision-making which may not be explicitly recorded in the data. The AI system can incorporate this knowledge into the learning process, allowing for a more accurate estimation of optimal actions in policy learning. This collaborative framework ensures that the learned policies better account for the missing confounders and yield more reliable and robust decision-making in practice.

We make the following contributions in the paper: We propose a novel algorithm for the problem of *deferral collaboration under unobserved confounding*, where our algorithm works

under a data-driven uncertainty set over the nominal propensity scores. The proposed algorithm leverages human decision-makers who have the capacity to acquire additional unrecorded information to aid their decision-making and a trained algorithmic policy. It offers policy improvement over a baseline policy only based on the available features. In addition, we propose a personalized variant of our algorithm that can route each instance to a specific human decision-maker by exploiting the diverse expertise of humans. We theoretically and empirically examine the efficacy of the proposed method.

## 2 Related Work

We consider human-AI collaboration as a decision-making problem in contrast to the predictive problem mostly considered by the extant human-AI systems. Related to policy learning on the observational data, we relax the untestable unconfoundedness assumption using sensitivity analysis from causal inference. The proposed human-AI algorithm is related to several threads of literature.

**Policy Learning from Observational Data with Unconfoundedness.** The challenge of deducing an optimal personalized policy from offline observational data has been extensively explored in various domains, including e-commerce, contextual pricing, and personalized medicine [12, 13, 14, 15, 16, 17, 18]. The majority of these studies assume that historical data were generated by a previous decision-maker, focusing on estimating treatment effects or determining an optimal algorithmic policy using proposed estimators and specific policy classes. Most research in this domain has not considered or developed learning algorithms for scenarios that could benefit from a combined human-AI team to enhance decision performance.

**Sensitivity Analysis.** Sensitivity analysis is applied to evaluate the assumptions that are not testable from the data in causal inference. Originating from the debate of smoking’s effect on lung cancer [19, 20], sensitivity analysis is often used to check the robustness of a causal conclusion under potentially unmeasured confounding. One direction of sensitivity analysis is to compute the influence of a latent confounding variable on the treatment and outcome variables using parametric models [21, 22, 23]. Another framework models the confounding effect on the treatment assignment nonparametrically. The seminal work of the Rosenbaum sensitivity model assumes the odds ratio of the treatment probability is bounded in an assumed range for a pair of units in the propensity score matching [24, 25]. The MSM generalizes this idea beyond matching algorithms. It assumes the odds ratio is bounded for a propensity score conditional on the observed variables and a true propensity score conditional on all the confounding variables [26, 27]. Due to its interpretability and minimal model assumptions, the MSM is widely adopted for heterogeneous treatment effect estimation [28, 29, 30], robust optimization [31, 32], policy evaluation [33], policy learning under unmeasured confounding [9] and selection bias [34]. In this paper, we adopt the MSM to quantify the deviation of unconfoundedness in the context of human-AI collaboration.

**Human-AI Collaboration.** Recent studies on human-AI collaboration methods have

explored ways to improve classification performance, such as accuracy and fairness, by capitalizing on the complementary strengths of humans and AI [35, 36, 37]. We focus on the setting without human-AI interaction, where decisions are made by either a human or an algorithm. Previous research has also addressed the task of routing instances to either a human or an algorithm [38, 39, 40, 41, 42]. [38, 39, 40] examine the optimization of overall classification performance, [41] investigates human-AI collaboration in a regression context, and [42] explores the simultaneous enhancement of human accuracy and fairness. The primary distinction between these studies and ours is that they explore contexts where the AI’s learning task is a conventional supervised classification task while we focus on policy learning. [4, 11] study how to design a deferral collaboration system similar to ours under the unconfoundness assumption, which assigns optimal decision maker (the human or the AI) for decision subjects to help make better decisions, based on the observational data. However, humans often leverage unrecorded information (unobserved confounders) to aid their decision making [10], which makes estimating the propensity scores in [4, 11] difficult.

### 3 Confounding-Robust Deferral Collaboration with Bandit Feedback

**Deferral Collaboration with Observational Data [4].** The observational data consist of the tuples  $\{X_i, T_i, Y_i\}_{i=1}^N$ , where the covariates  $X_i \in \mathcal{X}$ , the treatment arm  $T_i \in \{0, \dots, m-1\}$ , and a scalar outcome  $Y_i \in \mathbb{R}$ . The data is generated by the human decision maker with a behavior policy  $\pi_0$  as  $T_i \sim \text{Categorical}(\pi_0(T_i|X_i))$ . The behavior policy can be estimated from data. Using the potential outcome framework, we assume  $Y_i = Y_i(T_i)$ , *i.e.*, the potential outcome under the observed treatment equals the observed outcome, known as the SUTVA assumption [43]. We consider  $Y$  as the risk and aim to minimize the risk aggregated over the population. Deferral collaboration concerns how to evaluate and learn an algorithmic policy  $\pi : \mathcal{X} \rightarrow \Delta^m$  where the element in simplex  $\Delta^m$  is the probability over the treatment arms, along with a routing algorithm  $\phi : \mathcal{X} \rightarrow [0, 1]$  that can *complement* human decision-makers.  $\phi(X)$  denotes the probability of routing to humans.

A successful deferral collaboration routes different instances to the entity that is likely to yield the best reward by  $\phi(X)$ , and it leverages the policy  $\pi(x)$  for the instances routed to the AI. The human decision-maker may incur a cost of  $C(X)$  for producing a decision on an instance with features  $X$ .

The system is trained by optimizing the empirical estimate of the value function by inverse propensity weighting [1], using an estimated behavior policy  $\hat{\pi}_0$ ,

$$\min_{\phi \in \Phi, \pi \in \Pi} \sum_{i=1}^N \phi(X_i)(Y_i + C(X_i)) + \frac{(1 - \phi(X_i))\pi(T_i|X_i)}{\hat{\pi}_0(T_i|X_i)} Y_i. \quad (1)$$

At the testing time, a new decision instance will be routed to either human or the AI.

Equation (1) considers a single expert but in practice often there are multiple human decision-makers  $H \in \{1, \dots, K\}$ . Accordingly, the data is generated by first assigning an instance with covariates  $X_i$  to different human decision-makers by the assignment rule  $d_0(H_i|X_i) : \mathcal{X} \rightarrow \Delta^K$ . Each human decision-maker  $H_i$  chooses the treatment by the behavior policy  $\hat{\pi}_0(T_i|X_i, H_i)$ .

In this paper, we assume the system can route to a specific human decision-maker (personalization). The process is illustrated in Figure 1. The system is trained by optimizing

$$\min_{\phi \in \Phi, \pi \in \Pi} \sum_{i=1}^N \frac{\phi(H_i|X_i)}{d_0(H_i|X_i)} (Y_i + C(X_i)) + \frac{\phi(A|X_i)\pi(T_i|X_i)}{\hat{\pi}_0(T_i|X_i, H_i)} Y_i. \quad (2)$$

The routing algorithm  $\phi$  is generalized to a mapping  $\phi : \mathcal{X} \rightarrow \Delta^{K+1}$  where  $\phi(A|X), \phi(H|X)$  means the probability of routing instances to the algorithm and a specific human expert  $H$ . The goal is to learn an optimal routing algorithm  $\phi$  and policy  $\pi$  that minimizes the risk.

**Marginal Sensitivity Model.** We assume there is an unobserved feature  $U_i$ , which can be regarded as the unobserved potential outcome itself, *i.e.*,  $U_i = Y_i(t)$  [27]. The unconfoundedness assumption would hold if we account for both  $U_i$  and  $X_i$ . The nominal propensity is denoted as  $\tilde{\pi}_0(t|x) = P(T = t|X = x)$ , which can be estimated from the observational data using a classifier such as logistic regression. Due to the unobserved confounding, the true propensity (which cannot be estimated from data)  $\pi_0(t|x, y) = P(T = t|X = x, Y(t) = y)$  generally is not equal to the  $\tilde{\pi}_0(t|x)$ . To quantify the difference between the nominal and true propensity scores incurred by confounding, we consider an uncertainty set based on the odds-ratio bounds of the MSM [26],

$$\Gamma^{-1} \leq \frac{(1 - \tilde{\pi}_0(T|X)\pi_0(T|X, Y))}{\tilde{\pi}_0(T|X)(1 - \pi_0(T|X, Y))} \leq \Gamma, \quad (3)$$

where the scalar parameter  $\Gamma \geq 1$ . When  $\Gamma = 1$ , it corresponds to the unconfoundedness setup in Equation (1) and Equation (2).

### 3.1 Problem Statement

We first consider the situation of homogeneous human experts. We transform the expected team performance in Equation (1) to the self-normalized Hájek estimator [2] by

$$\begin{aligned} & \mathbb{E} \frac{\pi(T|X)}{\pi_0(T|X, Y)} Y (1 - d_\phi(X)) + \phi(X) (Y + C(X)) \\ & = \mathbb{E} \phi(X) (Y + C(X)) + \sum_{t=0}^{m-1} \frac{\mathbb{E} \frac{\mathbb{I}(T=t)}{\pi_0(T|X, Y)} \pi(T|X) Y (1 - \phi(X))}{\mathbb{E} \frac{\mathbb{I}(T=t)}{\pi_0(T|X, Y)}}. \end{aligned}$$

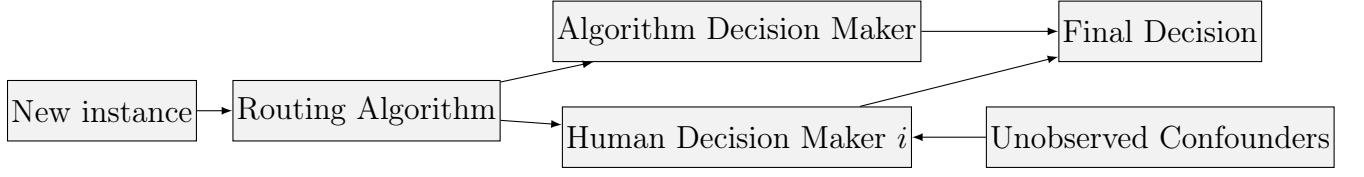


Figure 1: Decision-Making Process for Human-AI Collaboration with Unobserved Confounders.

Throughout the paper, without further specification, the expectation is with respect to the underlying data distribution. The equality is because  $\mathbb{E} \frac{\mathbb{I}(T=t)}{\pi_0(T|X,Y)} = 1$  for every  $t$ .

Suppose in addition there is a baseline policy  $\pi_c(T|X)$ , such as the never-treat policy  $\pi_c(0|x) = 1$ [9], that we aim to improve upon. The objective can be written as the improvement over  $\pi_c(T|X)$ ,

$$R(\pi, \phi, \pi_c) = \mathbb{E} \phi(X)(Y + C(X)) + \sum_{t=0}^{m-1} \frac{\mathbb{E} \frac{\mathbb{I}(T=t)}{\pi_0(T|X,Y)} Y [(1 - \phi(X))\pi(T|X) - \pi_c(t|X)]}{\mathbb{E} \frac{\mathbb{I}(T=t)}{\pi_0(T|X,Y)}}. \quad (4)$$

Let  $\tilde{W}_i = \frac{1}{\pi_0(T_i|X_i)}$  and  $W_i = \frac{1}{\pi_0(T_i|X_i, Y_i)}$ . By the MSM, a key observation is that the true weights  $W_i$  are in the uncertainty set  $\mathcal{W}_n^\Gamma = \{W : 1 + \Gamma^{-1}(\tilde{W}_i - 1) \leq W_i \leq 1 + \Gamma(\tilde{W}_i - 1), \forall i = 1, \dots, n\}$ . Hence, the worst-case empirical estimator  $\hat{R}_n(\pi, \phi, \pi_c, \mathcal{W}_n^\Gamma)$  equals

$$\begin{aligned} & \max_W \frac{1}{n} \sum_{i=1}^n \phi(X_i)(Y_i + C(X_i)) + \sum_{t=0}^{m-1} \frac{\frac{1}{n} \sum_i \mathbb{I}(T_i = t) [(1 - \phi(X_i))\pi(T_i|X_i) - \pi_c(T_i|X_i)] W_i Y_i}{\frac{1}{n} \sum_i \mathbb{I}(T_i = t) W_i} \\ & = \max_W \frac{1}{n} \sum_{i=1}^n \phi(X_i)(Y_i + C(X_i)) + \sum_{t=0}^{m-1} \frac{\frac{1}{n} \sum_i \mathbb{I}(T_i = t) [(1 - \phi(X_i))\pi(T_i|X_i) - \pi_c(T_i|X_i)] W_i Y_i}{\frac{1}{n} \sum_i \mathbb{I}(T_i = t) W_i} \\ & \quad s.t. \quad 1 + \Gamma^{-1}(\tilde{W}_i - 1) \leq W_i \leq 1 + \Gamma(\tilde{W}_i - 1), \end{aligned} \quad (5)$$

where  $W = (W_1, \dots, W_n)$ . The algorithm then chooses the policy and router that minimize the robust regret bound, where

$$\bar{\pi}(\Pi, \Phi, \pi_c, \mathcal{W}_n^\Gamma), \bar{\phi}(\Pi, \Phi, \pi_c, \mathcal{W}_n^\Gamma) = \arg \min_{\pi \in \Pi, \phi \in \Phi} \hat{R}_n(\pi, \phi, \pi_c, \mathcal{W}_n^\Gamma). \quad (6)$$

If we are interested in the policy improvement over the human's policy, we can optimize the future decision and routing policy by minimizing  $\hat{R}_n^H(\pi, \phi, \mathcal{W}_n^\Gamma)$  as

$$\max_W \frac{1}{n} \sum_{i=1}^n (\phi(X_i) - 1)(Y_i + C(X_i)) + \sum_{t=0}^{m-1} \frac{\frac{1}{n} \sum_i \mathbb{I}(T_i = t) [(1 - \phi(X_i)) \pi(T_i | X_i)] W_i Y_i}{\frac{1}{n} \sum_i \mathbb{I}(T_i = t) W_i}. \quad (7)$$

by removing the baseline policy  $\pi_c$  and comparing the future system's performance with the human's decision policy.

### 3.2 Personalization

In the collaborative objective mentioned earlier, we assume the experts have similar performance. However, this is not typically the case in real-world scenarios. Experts often possess different areas of expertise, and may get different levels of confounding information. For example, one general physician might excel at treating older patients with multiple health conditions by observing their bedside conditions, whereas another might only focus on recorded information. Therefore, implementing a personalized routing model could potentially enhance the performance of the human-machine team.

Rather than indiscriminately assigning an expert to evaluate a given instance, the routing algorithm can make a decision to either delegate the instance to an algorithm or to a human, and, more importantly, determine the most suitable human decision-maker for the task at hand accounting for varied degrees of confounding for each human. We assume the odds ratio of each human decision-maker  $H \in \{0, \dots, K-1\}$ 's propensity scores are associated with the confounding bound  $\Gamma_H$ . Similarly, the policy improvement with personalization has confounding-robust objective  $R_n^P(\pi, \phi, \pi_c, \mathcal{W}_n^{\Gamma_H})$  (as compared to the unconfounded version in Equation (2)) is

$$\begin{aligned} & \mathbb{E} \frac{\phi(a|X)\pi(T|X) - \pi_c(T|X)}{\pi_0(T|X, Y, H)} Y + \frac{\phi(H|X)}{d_0(H|X)} (Y + C(X)) \\ &= \mathbb{E} \sum_{t=0}^{m-1} \frac{\mathbb{I}(T=t)}{\pi_0(T|X, Y, H)} [\phi(a|X)\pi(T|X) - \pi_c(T|X)] Y + \mathbb{E} \frac{\phi(H|X)}{d_0(H|X)} (Y + C(X)) \\ &= \sum_{t=0}^{m-1} \frac{\mathbb{E} \frac{\mathbb{I}(T=t)}{\pi_0(T|X, Y, H)} [\phi(a|X)\pi(T|X) - \pi_c(T|X)] Y}{\mathbb{E} \frac{\mathbb{I}(T=t)}{\pi_0(T|X, Y, H)}} + \mathbb{E} \frac{\phi(H|X)}{d_0(H|X)} (Y + C(X)) \end{aligned} \quad (8)$$

Let  $\tilde{W}_i = \frac{1}{\tilde{\pi}_i(T_i|X_i, H_i)}$ ,  $W_i = \frac{1}{\pi_i(T_i|X_i, Y_i, H_i)}$ , then the worst-case estimator  $\hat{R}_n^P(\pi, \phi, \pi_c, \mathcal{W}_n^{\Gamma_H})$  is

$$\begin{aligned} & \max_W \sum_{t=0}^{m-1} \frac{\sum_i \mathbb{I}(T_i = t) W_i [\phi(a|X_i)\pi(T_i|X_i) - \pi_c(T_i|X_i)] Y_i}{\sum_i \mathbb{I}(T_i = t) W_i} + \frac{1}{n} \sum_{i=1}^n \frac{\phi(H_i|X_i)}{d_0(H_i|X_i)} (Y_i + C(X_i)) \quad (9) \\ & \text{s.t.} \quad 1 + \Gamma_{H_i}^{-1}(\tilde{W}_i - 1) \leq W_i \leq 1 + \Gamma_{H_i}(\tilde{W}_i - 1). \end{aligned}$$

The policy and router can be similarly found by optimizing the following objective,

$$\bar{\pi}(\Pi, \Phi, \pi_c, \mathcal{W}_n^{\Gamma_H}), \bar{\phi}(\Pi, \Phi, \pi_c, \mathcal{W}_n^{\Gamma_H}) = \arg \min_{\pi \in \Pi, \phi \in \Phi} \hat{R}_n^P(\pi, \phi, \pi_c, \mathcal{W}_n^{\Gamma_H}). \quad (10)$$

Compared to Equation (6), Equation (10) further considered how to leverage individual human expertise to minimize the human-AI team’s risk. It is easy to see that when the historical and future human assignment is fully randomized and each human decision maker has the same  $\Gamma$ , then Equation (10) recovers Equation (6).

## 4 Improvement Guarantee

In this section, we demonstrate that the worst-case empirical regret is an asymptotic upper bound for the true population regret. For the theoretical analysis, we assume the outcome and true propensity score is bounded, *i.e.*,  $|Y| \leq B, \pi_0(t|x, y) \geq v, \forall t \in \{0, \dots, m-1\}, x \in \mathcal{X}, y \in \mathcal{Y}$ . The following theorem guarantees the improvement over the population regret by solving the minimax optimization for the empirical regret.

**Theorem 1.** *Suppose the true inverse propensities  $1/\pi_0(T_i|X_i, Y_i) \in \mathcal{W}_n^\Gamma, i = 1, \dots, n$ ,  $|Y| \leq B, \pi_0(t|x, y) \geq v, \forall t \in \{0, \dots, m-1\}, x \in \mathcal{X}, y \in \mathcal{Y}$  and denote policy and router’s class  $\Pi$  and  $\Phi$ ’s Rademacher Complexity as  $\mathfrak{R}_n(\Pi)$  and  $\mathfrak{R}_n(\Phi)$ , then for  $\delta > 0$ , with probability  $1 - \delta$ , we have*

$$R(\pi, \phi, \pi_c) \leq \hat{R}_n(\pi, \phi, \pi_c, \mathcal{W}_n^\Gamma) + (3B + 3\bar{c} + \frac{5B + 1}{\nu^2}) \sqrt{\frac{2 \log \frac{8m}{\delta}}{n}} + 2\frac{B}{\nu} \mathfrak{R}_n(\Pi) + 2(B + \bar{c}) \mathfrak{R}_n(\Phi)$$

The proof is included in Appendix A and can be easily extended for the improvement guarantee over the human policy and of the personalized version of the algorithm. Note that the global optima of the empirical objective is never positive when  $\pi_c \in \Pi$  since we can take  $\pi = \pi_c$  and  $\phi(X) = 0$ . If we only consider  $\Pi, \Phi$  with vanishing Rademacher Complexity (*i.e.*,  $O(n^{-1/2})$ ), then Theorem 1 implies that given enough samples, if the empirical objective is negative, we can get some improvement over  $\pi_c$  under well-specification.

**Data-Driven Calibration of  $\Gamma$ .** Since the theorem assumes well-specification, the practitioner needs to specify a plausible strength of the unmeasured confounding by the confounding strength parameter  $\Gamma$ . Though the exact value of  $\Gamma$  involves the true propensity score that is not identifiable from the data, we can have a reference point by quantifying the impact of the observed covariates on the propensity score. The parameter  $\Gamma$  defined in Equation (3) measures the degree of influence of the confounder  $U = Y(t)$  on the propensity odds. Similarly, following [44, 45, 23], we measure the impact of an observed covariate  $Z$  given the other observed covariates  $X \setminus Z$ . The reference points of  $\Gamma$  is computed from the odds ratio  $\frac{(1-\bar{\pi}_0(T|X \setminus Z)\bar{\pi}_0(T|X))}{\bar{\pi}_0(T|X \setminus Z)(1-\bar{\pi}_0(T|X))}$ . The covariate  $Z$  can also be a group of correlated observed variables that better mimic the nature of unmeasured confounding variables [23]. We refer to [45] for a detailed discussion on potential conservatism in this calibration procedure.



## 5 Optimizing Confounding-Robust Deferral Collaboration System

We next discuss how to optimize the deferral collaboration system in Equation (6) and Equation (10). First, we need to solve the inner maximization in Equation (5) and Equation (9).

To simplify notations, we consider the following optimization problem

$$\hat{Q}_t(r, \mathcal{W}) = \max_{W \in \mathcal{W}} \frac{\sum_{i=1}^n r_i W(T_i, X_i, Y_i)}{\sum_{i=1}^n W(T_i, X_i, Y_i)} \quad \text{s.t.} \quad a_i^{\Gamma_i} \leq W(T_i, X_i, Y_i) \leq b_i^{\Gamma_i} \quad (11)$$

When  $r_i = \mathbb{I}(T_i = t)[(1 - \phi(X_i))\pi(T_i|X_i) - \pi_c(T_i|X_i)]Y_i$ ,  $a_i^{\Gamma_i} = 1 + \Gamma^{-1}(\tilde{W}_i - 1)$ ,  $b_i^{\Gamma_i} = 1 + \Gamma(\tilde{W}_i - 1)$ , solving Equation (11) is equivalent to optimizing  $W$  for the empirical  $\hat{R}_n(\pi, \phi, \pi_c, \mathcal{W}_n^\Gamma)$  in Equation (5), and when  $r_i = \mathbb{I}(T_i = t)[\phi(a|X_i)\pi(T_i|X_i) - \pi_c(T_i|X_i)]Y_i$ ,  $a_i^{\Gamma_i} = 1 + \Gamma_{H_i}^{-1}(\tilde{W}_i - 1)$ ,  $b_i^{\Gamma_i} = 1 + \Gamma_{H_i}(\tilde{W}_i - 1)$ , solving Equation (11) is equivalent to optimizing  $W$  for  $\hat{R}_n^P(\pi, \phi, \pi_c, \mathcal{W}_n^{\Gamma_H})$  in Equation (9).

The optimization problem in Equation (11) is known to be a *linear fractional program* [46, 9, 30, 28]. Taking the derivative of the objective in Equation (11) w.r.t.  $W_i = W(T_i, X_i, Y_i)$ , the objective is monotonically increasing (decreasing) with  $W_i$  if  $r_i \sum_{j \neq i} W_j - \sum_{j \neq i} r_j W_j$  is greater (less) than zero. Hence the optima is achieved when all the  $W_i$  are taking the value at the boundary. Furthermore, the objective can be viewed as a weighted combination of  $r_i$  with the weights adding up to one. So the objective is maximized when the weights  $W_i / \sum_i W_i$  are high for the large  $r_i$  and are low for the small  $r_i$ . Based on these insights, the optimal weights  $\{W_i\}$  of the linear fractional program can be characterized by the following theorem.

**Theorem 2.** *Let  $(i)$  be the ordering such that  $r_{(1)} \leq r_{(2)} \leq \dots \leq r_{(n)}$ .  $\hat{Q}_t(r, \mathcal{W}) = \lambda(k^*)$ , where  $k^* = \inf\{k = 1, \dots, n+1 : \lambda(k) < \lambda(k-1)\}$  and*

$$\lambda(k) = \frac{\sum_{i < k} a_{(i)}^{\Gamma_{(i)}} r_{(i)} + \sum_{i \geq k} b_{(i)}^{\Gamma_{(i)}} r_{(i)}}{\sum_{i < k} a_{(i)}^{\Gamma_{(i)}} + \sum_{i \geq k} b_{(i)}^{\Gamma_{(i)}}} \quad (12)$$

See Appendix A for the proof. Theorem 2 provides an efficient way to solve Equation (11) by line search: first sort  $r_i$  in ascending order and initialize all  $W_i = a_i^\Gamma$ , then change  $W_k$  to  $b_k^\Gamma$  for  $k = n, n-1, \dots, 1$  until the first time when  $\lambda(k)$  decreases.

After solving the inner maximization problem, we can proceed to optimize the minimization problem in Equation (6) and Equation (10). In this paper, we consider differentiable policies  $\Pi = \{\pi_\theta : \theta \in \Theta\}$  and router class  $\Phi = \{\phi_\rho, \rho \in \mathcal{P}\}$ , such as logistic policies with  $\pi_{\{\alpha, \beta\}}(x) = \sigma(\alpha + \beta^T x)$  or neural networks, so the following optimization problem can be efficiently solved by gradient descent. For every iteration, our algorithm starts by finding the weights  $W$  given the current model parameters through line search, then uses gradient descent to update policy and router jointly. We refer to our main algorithm assuming all

decision makers can only be queried randomly as ConfHAI and its variant considering the diverse expertise of individual human decision makers as ConfHAIPerson. The algorithm is summarized in Algorithm 1.

---

**Algorithm 1** Confounding-Robust Deferral Collaboration (ConfHAI/ConfHAIPerson)

---

**Input:** number of iterations  $N$

**Output:**  $\pi_\theta, \phi_\rho$

**for**  $i \leftarrow 1$  to  $N$  **do**

$W \leftarrow \arg \max_{W \in \mathcal{W}}$  Equation (5) (Equation (9) for ConfHAIPerson).

$\theta, \rho \leftarrow \nabla \hat{R}_n(\pi, \phi, \pi_c, \mathcal{W}_n^\Gamma)$  ( $\nabla \hat{R}_n^P(\pi, \phi, \pi_c, \mathcal{W}_n^{\Gamma_H})$  for ConfHAIPerson).

**end for**

---

## 6 Experiments

In this section, we report empirical findings from two experiments conducted to examine the advantages of being robust to unobserved confounding. Our initial experiment involves a synthetic example used in [47], which we employ to demonstrate the benefit of human-AI collaboration within a controlled environment. Our subsequent experiment establishes two real-world examples in financial lending and healthcare scenarios where human-AI collaboration can be implemented.

In our experiment, we examine the following decision-making configurations. For all baseline scenarios that don't involve personalization, human experts are selected at random. Human Only (Human) solely queries human-decision-makers randomly to output final decisions. Algorithm Only (AO) uses the inverse propensity score weighting method [18] to train a policy. Confounding-Robust Algorithm Only (ConfAO) trains a confounding-robust policy [47] to determine the final decisions. Human-AI team (HAI) uses the deferral collaboration method proposed in [4] to train a router and policy jointly assuming unconfoundness. Our method and its personalized variant are denoted as ConfHAI and ConfHAIPerson respectively. See Appendix B for a more detailed discussion about the baselines. We use the logistic policies [47] for the policy and router model classes. The baseline policy is the never-treat policy  $\pi_c(0|x) = 1$  following [47, 9].

### 6.1 Synthetic Experiment

We use the synthetic example described in [9] to demonstrate the benefit of human-AI team performance with potential confounding.

$$\xi \sim \text{Bernoulli}(0.5), X \sim \mathcal{N}((2\xi - 1)\mu_x, I_5), U = \mathbb{I}[Y_i(1) < Y_i(-1)]$$

$$Y(t) = \beta_0^T x + \mathbb{I}[t = 1]\beta_{\text{treat}}^T x + 0.5\alpha\xi\mathbb{I}[t = 1] + \eta + w\xi + \epsilon$$

where  $\beta_{\text{treat}} = [1.5, 1, 1.5, 1, 0.5]$ ,  $\mu_x = [1, .5, 1, 0, 1]$ ,  $\eta = 2.5$ ,  $\alpha = -2$ ,  $w = 1.5$  and  $\epsilon \sim \mathcal{N}(0, 1)$ . The nominal propensity  $\pi_0(T = 1|X) = \sigma(\beta^T X)$  and  $\beta = [0, .75, .5, 0, 1, 0]$ ,  $T_i$  is then generated according to true propensities by  $\pi_0(T = 1|X, U) = \frac{(\Gamma U + 1 - U)\pi_0(T=1|X)}{[1 + 2(\Gamma - 1)\pi_0(T=1|X) - \Gamma]U + \Gamma + (1 - \Gamma)\pi_0(T=1|X)}$ , where  $\Gamma$  is the specified level of confounding. In this setting, the human decision maker will acquire unobserved information to improve their decisions, similar to [47, 9], we set  $\log(\Gamma) = 2.5$  and  $C(x) = 0$ . We vary the confounding parameter in  $\{0.01, 0.5, 1, 1.5, 2, 2.5, 3, 3.5, 4\}$ . To also test the personalized variant, we simulate three human decision makers with the same  $\Gamma$  in this setting.

The results are shown in Figure 2a. The baselines do not consider unobserved confounding have similar performance with our methods and ConfAO when  $\Gamma$  is small, which assumes small confoundness. When  $\Gamma$  is approaching the underlying confounding factor, we observe a significant policy improvement over the baseline policy (regret is smaller than 0). The personalized method achieves similar performance compared to ConfHAI since all human decision makers have the same performance here. In this example, interestingly, the ConfAO policy is actually worse than humans’ performance, and almost never exceeds humans’ performance with varying  $\Gamma$ , while human-AI complementarity is still possible with our proposed methods under correctly specified and large  $\Gamma$ , which emphasizes the benefit of our proposed confounding-robust deferral system.

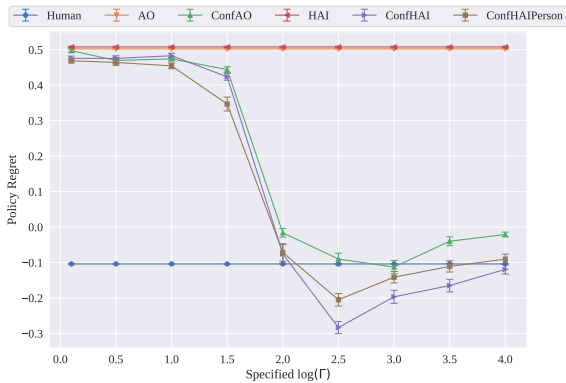
Next, we simulate three human workers with  $\log(\Gamma) = 1, 2.5, 4$  respectively, which corresponds to the setting where different humans may acquire different unobserved information to aid their decision making and some expert workers may demonstrate better performance than their peers. We examine four  $\Gamma$  specifications with heterogeneous workers:  $[1, 1, 1]$ ,  $[2.5, 2.5, 2.5]$ ,  $[1, 2.5, 4]$ ,  $[4, 4, 4]$  and show the results in Figure 2b. With small  $\Gamma$  (a weak unmeasured confounding), similarly, we observe all methods perform suboptimally with no policy improvement. The personalized variant has an additional improvement over ConfHAI by leveraging the diverse expertise of human decision makers. With correctly specified and relatively large  $\Gamma$ , we observe that ConfHAI and ConfHAIPerson significantly outperform other baselines and demonstrate human-AI complementarity, where they outperform both human-only and algorithm-only teams.

## 6.2 Real-World Examples

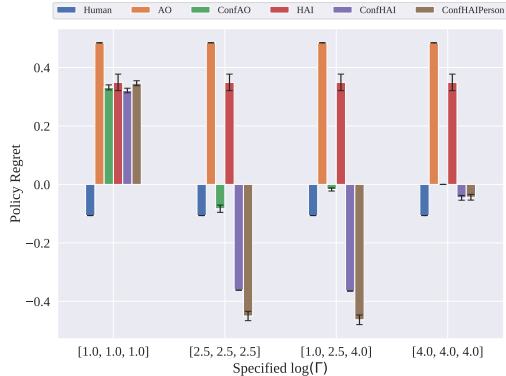
We provide two real-world examples in this section to help readers better understand our methods. We set  $C(x) = 0.1$  for both examples. See Appendix C for more details about the datasets and training details in the experiments due to space constraints.

**Financial Lending.** Consider a financial leading setup, where loan officers can obtain additional information by visiting the loan applicants and improving their decision-making. However, due to the unexpected scenarios the loan officers may encounter, such information was not recorded in the historical data. We use the Home Equity Line of Credit(HELOC)<sup>1</sup>

<sup>1</sup><https://community.fico.com/s/explainable-machine-learning-challenge>



(a) Policy regret with homogeneous humans.



(b) Policy regret with heterogeneous humans.

Figure 2: Policy Regret for Different Methods. ConfHAI and ConfHAIPerson offer consistent and significantly better policy improvement with correct and large  $\Gamma$  compared to algorithm only baselines. When  $\Gamma$  is small, they perform similarly to baseline methods assuming unconfoundedness.

dataset which contains anonymized information about credit applications by real homeowners. Some of the used features include average months since the account opened, maximum delinquency, and number of inquiries in the last 6 months. We assume there are three human decision makers with  $\log(\Gamma) = [0.1, 0.1, 1]$ , which means two of them rarely seek external information to improve their decision making and another decision maker is more likely to get external risk estimation when evaluating applications. We train a logistic regression on 10% of the data to simulate nominal policies, which can be a guideline policy of the insurance company, and the actual treatments taken is generated using the same procedure in Section 6.1 and the fitted nominal propensity is estimated using logistic regression on actual treatments. The outcome of the dataset is a binary outcome indicating whether the applicant was 90 days past due since the account was opened over 24 months. We build a risk function where the loan company will receive a risk  $Y \sim \mathcal{N}(0, 1)$  if not approving the loan,  $Y \sim \mathcal{N}(-2, 1)$  if approving for an applicant with good credit and  $Y \sim \mathcal{N}(2, 1)$  if approving for an applicant with bad credit.

**Acute Stroke Treatment.** Consider another healthcare example built in [47] where the doctors need to treat patients with acute stroke. In this case, experienced doctors may observe bedside information, and past patient behaviors to aid their decision-making, which are not recorded in the historical records. We use the data from the International Stroke Trial [48] and focus on two treatment arms: the treatment of both aspirin and heparin (medium and high doses), and the treatment of aspirin only. Since the trial only has the outcome under action taken, we create potential outcomes by fitting a separate random forest model for each treatment as in [8, 49]. The outcome is a composite score including variables like death, recurrent stroke, pulmonary embolism, and recovery. Some of the features used by the algorithm include age, sex, deficient symptoms, stroke types, and cerebellar signs. Similarly,

we assume there are three human physicians with  $\log(\Gamma) = [0.1, 0.1, 1]$  prescribing treatments. The results are shown in Figure 3a and Figure 3b respectively. For each experiment, we try three  $\log(\Gamma)x$  specifications:  $[0.1, 0.1, 0.1]$ ,  $[0.1, 0.1, 1]$  and  $[1, 1, 1]$ , which correspond to under, correct and over specifications. In HELOC, the baselines not considering unobserved confounding can still achieve policy improvement, while it is not consistent across settings, *e.g.*, in IST. We observe that ConfHAI and ConfHAIPerson achieve the best performance with correctly-specified  $\Gamma$  and the personalized variant achieves significantly better performance than other methods. With over-specification, the performance of confounding-robust methods decreases but can reliably provide policy improvement. Similarly, ConfAO can provide policy improvement with different specifications of  $\Gamma$ , however, its performance is often much worse than the human-AI methods we propose.

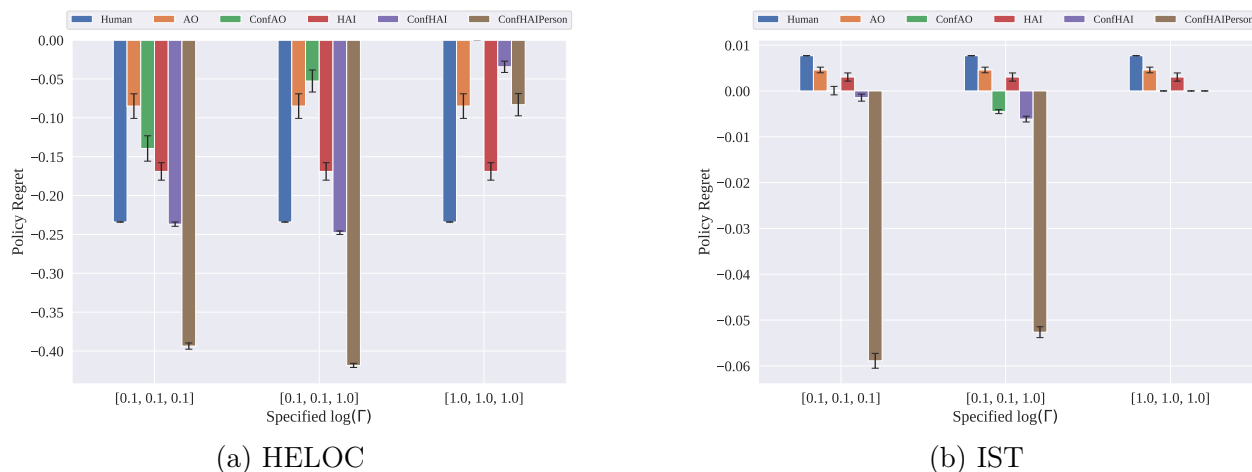


Figure 3: Policy Regret with Real-World Examples. In HELOC and IST, we find that the ConfHAI and ConfHAIPerson can offer policy improvement (negative regret) under different  $\Gamma$  specifications while the benefit is the largest with the correct specification. The proposed methods achieve significantly better performance compared to ConfAO and more robust performance with respect to unobserved confounding compared to baselines assuming unconfoundness.

### 6.3 Real Human Responses

In addition, we use the real human responses to validate our approach. We use the scientific annotation dataset FOCUS [50, 4] with responses from five human annotators. We assume if the human annotator considers the sentence scientific, they will apply action I (*e.g.*, retweet the paper), if the sentence is indeed scientific, the risk is  $\mathcal{N}(-1, 1)$ , otherwise the risk is from  $\mathcal{N}(1, 1)$ . On the other hand, if the human annotator considers the sentence as non-scientific, they will apply action II (*e.g.*, ignore the paper), if the sentence is indeed non-scientific, the risk is  $\mathcal{N}(-1, 1)$  (otherwise the risk is  $\mathcal{N}(1, 1)$ ).

The confounding is created by removing samples with 20% top outcomes in the treated group and 20% bottom outcomes in the control group following [47]. We specify the same  $\Gamma$  for each human decision maker and vary it.

The results are shown in Figure 4. This dataset is different from our simulations since humans’ true propensities may not reflect the worst case indicated in the MSM optimization. However, we still observe our methods consistently offer the best performance with a wide range of  $\Gamma$ .

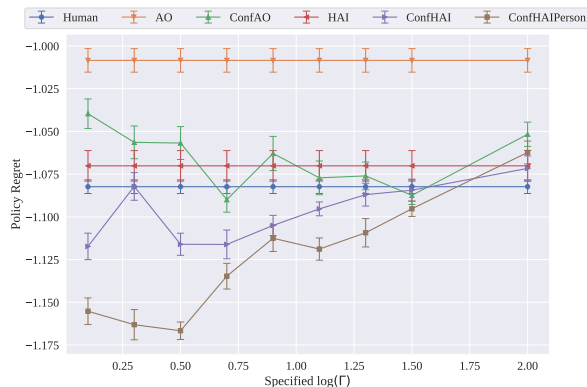


Figure 4: Results with Real Human Responses. We still observe our methods consistently offer the best performance with a wide range of  $\Gamma$ .

## 6.4 Ablation Studies

We also examine the effect of human cost on the risk of each method. We use the synthetic data setup and vary the human cost from 0 to 0.3. Since the human’s cost becomes higher, the Human baseline’s performance gets worse. Human-AI systems’ performance (HAI, ConfHAI, ConfHAIPerson) is also impacted when human cost is higher, but the proposed methods consistently outperform other baselines.

## 7 Conclusion and Future Work

In this paper, we propose a novel approach to the confounding-robust policy improvement problem within Human-AI team settings. The algorithms we developed aim to optimize policy decisions by selectively deferring decision instances to either humans or the AI, based on the context and capabilities of both. Our results indicate that the proposed models exhibit promise in achieving robust policy improvements, providing a foundation for future work in this area.

Despite the encouraging results, this work is not without its limitations. The most substantial limitation is the absence of real human studies. While our algorithm has been designed with

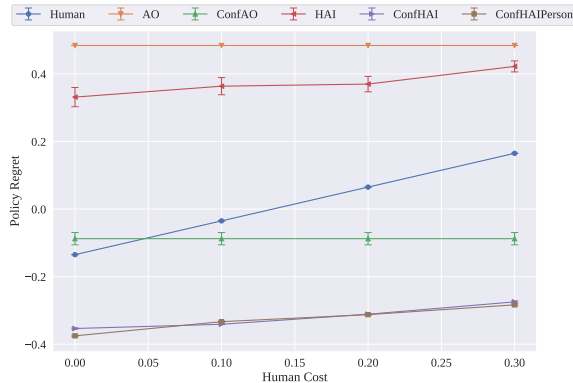


Figure 5: Ablation Study for Human Cost on Synthetic Data.

human decision-making in mind, the lack of empirical validation with real human subjects is a significant gap. Future work should therefore incorporate user studies to validate and refine the model based on actual human behavior and decision-making processes. Another limitation lies in the relatively strict constraints on the marginal sensitivity model. These constraints may limit the generalizability and applicability of our approach in certain complex decision-making environments. As such, further research is necessary to explore and develop methods for relaxing these constraints without sacrificing the robustness of policy improvement.

In conclusion, we believe that our work presents an important step forward in the field of Human-AI teams and confounding-robust policy improvement. It opens up new possibilities for future research and practical applications, particularly in terms of how humans and AI can work together more effectively to improve policy decisions. We anticipate that subsequent research will build upon our work, conducting human studies and refining the approach to overcome the identified limitations. We are optimistic about the potential of this line of inquiry to drive significant advancements in policy-making processes in the years to come.

## References

- [1] Susan Athey and Stefan Wager. Policy learning with observational data. *Econometrica*, 89(1):133–161, 2021.
- [2] Adith Swaminathan and Thorsten Joachims. The self-normalized estimator for counterfactual learning. *advances in neural information processing systems*, 28, 2015.
- [3] Thorsten Joachims, Adith Swaminathan, and Maarten de Rijke. Deep learning with logged bandit feedback. In *ICLR*, 2018.
- [4] Ruijiang Gao, Maytal Saar-Tsechansky, Maria De-Arteaga, Ligong Han, Min Kyung Lee, and Matthew Lease. Human-ai collaboration with bandit feedback. *arXiv preprint arXiv:2105.10614*, 2021.

- [5] Nathan Kallus. More efficient policy learning via optimal retargeting. *Journal of the American Statistical Association*, 116(534):646–658, 2021.
- [6] Donald B Rubin. Estimating causal effects of treatments in randomized and nonrandomized studies. *Journal of educational Psychology*, 66(5):688, 1974.
- [7] Léon Bottou, Jonas Peters, Joaquin Quiñero-Candela, Denis X Charles, D Max Chickering, Elon Portugaly, Dipankar Ray, Patrice Simard, and Ed Snelson. Counterfactual reasoning and learning systems: The example of computational advertising. *Journal of Machine Learning Research*, 14(11), 2013.
- [8] Max Biggs, Ruijiang Gao, and Wei Sun. Loss functions for discrete contextual pricing with observational data. *arXiv preprint arXiv:2111.09933*, 2021.
- [9] Nathan Kallus and Angela Zhou. Minimax-optimal policy learning under unobserved confounding. *Management Science*, 67(5):2870–2890, 2021.
- [10] Kenneth Holstein, Maria De-Arteaga, Lakshmi Tumati, and Yanghui Cheng. Toward supporting perceptual complementarity in human-ai collaboration via reflection on unobservables. *Proceedings of the ACM on Human-Computer Interaction*, 7(CSCW1):1–20, 2023.
- [11] Ruijiang Gao, Maytal Saar-Tsechansky, Maria De-Arteaga, Ligong Han, Wei Sun, Min Kyung Lee, and Matthew Lease. Learning complementary policies for human-ai teams. *arXiv preprint arXiv:2302.02944*, 2023.
- [12] Miroslav Dudík, Dumitru Erhan, John Langford, and Lihong Li. Doubly robust policy evaluation and optimization. *Statistical Science*, 29(4):485–511, 2014.
- [13] Susan Athey and Stefan Wager. Efficient policy learning. Technical report, 2017.
- [14] Nathan Kallus. Balanced policy evaluation and learning. *Advances in neural information processing systems*, 31, 2018.
- [15] Nathan Kallus. Classifying treatment responders under causal effect monotonicity. In *International Conference on Machine Learning*, pages 3201–3210. PMLR, 2019.
- [16] Ruijiang Gao, Max Biggs, Wei Sun, and Ligong Han. Enhancing counterfactual classification via self-training. *arXiv preprint arXiv:2112.04461*, 2021.
- [17] Arjun Sondhi, David Arbour, and Drew Dimmery. Balanced off-policy evaluation in general action spaces. In *International Conference on Artificial Intelligence and Statistics*, pages 2413–2423. PMLR, 2020.
- [18] Adith Swaminathan and Thorsten Joachims. Counterfactual risk minimization: Learning from logged bandit feedback. In *ICML*, pages 814–823, 2015.



- [19] Jerome Cornfield, William Haenszel, E Cuyler Hammond, Abraham M Lilienfeld, Michael B Shimkin, and Ernst L Wynder. Smoking and lung cancer: recent evidence and a discussion of some questions. *Journal of the National Cancer institute*, 22(1):173–203, 1959.
- [20] Ronald Fisher. Cigarettes, cancer, and statistics. *The Centennial Review of Arts & Science*, 2:151–166, 1958.
- [21] Guido W Imbens. Sensitivity to exogeneity assumptions in program evaluation. *American Economic Review*, 93(2):126–132, 2003.
- [22] Paul R Rosenbaum. Sensitivity analysis for certain permutation inferences in matched observational studies. *Biometrika*, 74(1):13–26, 1987.
- [23] Victor Veitch and Anisha Zaveri. Sense and sensitivity analysis: Simple post-hoc analysis of bias due to unobserved confounding. In *Advances in Neural Information Processing Systems*, volume 33, pages 10999–11009, 2020.
- [24] Paul R Rosenbaum. Sensitivity analysis in observational studies. *Encyclopedia of Statistics in Behavioral Science*, 2005.
- [25] Paul R. Rosenbaum. *Observational Studies (2nd ed.)*. Springer, New York, 2002.
- [26] Zhiqiang Tan. A distributional approach for causal inference using propensity scores. *Journal of the American Statistical Association*, 101(476):1619–1637, 2006.
- [27] Q Zhao, D Small, and B Bhattacharya. Sensitivity analysis for inverse probability weighting estimators via the percentile bootstrap. *Journal of the Royal Statistical Society: Series B (Statistical Methodology)*, 81(4):735–761, 2019.
- [28] Ying Jin, Zhimei Ren, and Emmanuel J Candès. Sensitivity analysis of individual treatment effects: A robust conformal inference approach. November 2021.
- [29] Steve Yadowsky, Hongseok Namkoong, Sanjay Basu, John Duchi, and Lu Tian. Bounds on the conditional and average treatment effect with unobserved confounding factors. *arXiv preprint arXiv:1808.09521*, 2018.
- [30] Mingzhang Yin, Claudia Shi, Yixin Wang, and David M Blei. Conformal sensitivity analysis for individual treatment effects. *arXiv preprint arXiv:2112.03493*, 2021.
- [31] Hongseok Namkoong, Yuanzhe Ma, and Peter W Glynn. Minimax optimal estimation of stability under distribution shift. December 2022.
- [32] Wenshuo Guo, Mingzhang Yin, Yixin Wang, and Michael Jordan. Partial identification with noisy covariates: A robust optimization approach. In *Conference on Causal Learning and Reasoning*, pages 318–335. PMLR, 2022.

- [33] Hongseok Namkoong, Ramtin Keramati, Steve Yadlowsky, and Emma Brunskill. Off-policy policy evaluation for sequential decisions under unobserved confounding. *Advances in neural information processing systems*.
- [34] Lihua Lei, Roshni Sahoo, and Stefan Wager. Policy learning under biased sample selection. *arXiv preprint arXiv:2304.11735*, 2023.
- [35] Gagan Bansal, Besmira Nushi, Ece Kamar, Dan Weld, Walter Lasecki, and Eric Horvitz. A case for backward compatibility for human-ai teams. *arXiv preprint arXiv:1906.01148*, 2019.
- [36] Rouba Ibrahim, Song-Hee Kim, and Jordan Tong. Eliciting human judgment for prediction algorithms. *Management Science*, 67(4):2314–2325, 2021.
- [37] Nicholas Wolczynski, Maytal Saar-Tsechansky, and Tong Wang. Learning to advise humans by leveraging algorithm discretion. *arXiv:2210.12849*, 2022.
- [38] David Madras, Toni Pitassi, and Richard Zemel. Predict responsibly: improving fairness and accuracy by learning to defer. *NeurIPS*, 31:6147–6157, 2018.
- [39] Bryan Wilder, Eric Horvitz, and Ece Kamar. Learning to complement humans. *arXiv*, 2020.
- [40] Maithra Raghu, Katy Blumer, Greg Corrado, Jon Kleinberg, Ziad Obermeyer, and Sendhil Mullainathan. The algorithmic automation problem: Prediction, triage, and human effort. *arXiv:1903.12220*, 2019.
- [41] Abir De, Paramita Koley, Niloy Ganguly, and Manuel Gomez-Rodriguez. Regression under human assistance. In *AAAI*, pages 2611–2620, 2020.
- [42] Tong Wang and Maytal Saar-Tsechansky. Augmented fairness: An interpretable model augmenting decision-makers’ fairness. *arXiv:2011.08398*, 2020.
- [43] Donald B Rubin. Randomization analysis of experimental data: The fisher randomization test comment. *Journal of the American statistical association*, 75(371):591–593, 1980.
- [44] Jesse Y Hsu and Dylan S Small. Calibrating sensitivity analyses to observed covariates in observational studies. *Biometrics*, 69(4):803–811, 2013.
- [45] Carlos Cinelli and Chad Hazlett. Making sense of sensitivity: Extending omitted variable bias. *Journal of the Royal Statistical Society: Series B (Statistical Methodology)*, 82(1):39–67, 2020.
- [46] SS Chadha and Veena Chadha. Linear fractional programming and duality. *Central European Journal of Operations Research*, 15:119–125, 2007.
- [47] Nathan Kallus and Angela Zhou. Confounding-robust policy improvement. In *NeurIPS*, pages 9269–9279, 2018.

- [48] International Stroke Trial Collaborative Group. The international stroke trial (ist): a randomised trial of aspirin, subcutaneous heparin, both, or neither among 19 435 patients with acute ischaemic stroke. *The Lancet*, 349(9065):1569–1581, 1997.
- [49] Adam Elmachtoub, Vishal Gupta, and Yunfan Zhao. Balanced off-policy evaluation for personalized pricing. In *International Conference on Artificial Intelligence and Statistics*, pages 10901–10917. PMLR, 2023.
- [50] Andrey Rzhetsky, Hagit Shatkay, and W John Wilbur. How to get the most out of your curation effort. *PLoS computational biology*, 5(5):e1000391, 2009.
- [51] Michel Ledoux and Michel Talagrand. *Probability in Banach Spaces: isoperimetry and processes*, volume 23. Springer Science & Business Media, 1991.

## A Proofs

Proof of Theorem 1:

*Proof.* Assume  $|Y| \leq B, W \leq 1/\nu$ . Let  $\hat{D}_t = \mathbb{E}_n[W^* \mathbb{1}(T = t)]$ . With some abuse of notations, we use  $\hat{R}(\pi, \phi, \pi_c, \mathcal{W}^*)$  to represent the empirical estimator with the optimal weight  $W^*$ .

$$\sup_{\pi \in \Pi, \phi \in \Phi} R(\pi, \phi, \pi_c) - \hat{R}(\pi, \phi, \pi_c, \mathcal{W}^*) \quad (13)$$

$$= \sup_{\pi \in \Pi, \phi \in \Phi} -\frac{1}{n} \sum_i \phi(X_i)(Y_i + C(X_i)) + \mathbb{E}\phi(X)(Y + C(X)) \quad (14)$$

$$- \frac{1}{n} \frac{\sum_i (\pi(T_i|X_i)(1 - \phi(X_i)) - \pi_c(T_i|X_i, U_i)) W_i Y_i}{\mathbb{E}\hat{D}_{T_i}} \left( \frac{\mathbb{E}\hat{D}_{T_i} - \hat{D}_{T_i}}{\hat{D}_{T_i}} + 1 \right) \quad (15)$$

$$+ \mathbb{E}(\pi(T|X)(1 - \phi(X)) - \pi_c(T|X, U)) W Y \quad (16)$$

$$\leq \sup_{\phi \in \Phi} -\frac{1}{n} \sum_i \phi(X_i)(Y_i + C(X_i)) + \mathbb{E}\phi(X)(Y + C(X)) \quad (17)$$

$$+ \sup_{\pi \in \Pi, \phi \in \Phi} (\mathbb{E}_n - \mathbb{E})(\pi(T|X)(1 - \phi(X)) - \pi_c(T|X, U)) W Y + \frac{B}{\nu} \sum_i \frac{1}{n} \frac{\mathbb{E}\hat{D}_{T_i} - \hat{D}_{T_i}}{\hat{D}_{T_i}} \quad (18)$$

Write

$$D = \sup_{\phi \in \Phi} \left\{ -\frac{1}{n} \sum_i \phi(X_i)(Y_i + C(X_i)) + \mathbb{E}\phi(X)(Y + C(X)) \right\}, \quad (19)$$

Since it has bounded difference of  $\frac{B+\bar{c}}{n}$ , McDiarmid' inequality indicates with probability  $1 - p_1$ ,

$$D - \mathbb{E}D \leq (B + \bar{c})\sqrt{\frac{\log \frac{1}{p_1}}{2n}} \quad (20)$$

By the standard symmetrization method, we have

$$\mathbb{E}D \leq 2\mathbb{E} \sup_{\phi \in \Phi} \sum_i^n \epsilon_i [\phi(X_i)(Y_i + C(X_i))] \quad (21)$$

By Rademacher comparison theorem / contraction principle [51],

$$\mathbb{E}D \leq 2(B + \bar{c})\mathbb{E}\mathfrak{R}_n(\Phi) \quad (22)$$

Next we bound  $\frac{B}{\nu} \sum_i \frac{1}{n} \frac{\mathbb{E}\hat{D}_{T_i} - \hat{D}_{T_i}}{\hat{D}_{T_i}}$ . Let  $n_t = \sum_i \mathbb{1}[T_i = t]$ ,

$$\frac{B}{\nu} \sum_i \frac{1}{n} \frac{\mathbb{E}\hat{D}_{T_i} - \hat{D}_{T_i}}{\hat{D}_{T_i}} \leq \frac{B}{n\nu} \sum_t \frac{|\hat{D}_t - 1|}{\hat{D}_t} \quad (23)$$

For any  $t$ , write  $\rho_t = P(T = t)$ , by Hoeffding inequality,

$$P(|\frac{n_t}{n} - \rho_t| \geq \rho_t/2) \leq 2 \exp(-\nu^2 \rho_t^2 n/2) \quad (24)$$

Take a union bound over  $m$  treatments, with probability  $p_2$ , such that  $\frac{1}{\nu} \sqrt{\frac{\log(2m/p_2)}{2n}} \leq \rho_t^2/2$ .

Again with Hoeffding inequality,

$$P(|\hat{D}_t - 1| \geq \epsilon) \leq 2 \exp(-2\nu^2 \epsilon^2 n) \quad (25)$$

With  $p_3$ , such that  $\frac{1}{\nu} \sqrt{\frac{\log(2m/p_3)}{2n}} \leq 1$ , thus with  $1 - p_3$ ,  $\frac{1}{\hat{D}_t} \leq 2$  and  $\frac{|\hat{D}_t - 1|}{\hat{D}_t} \leq \frac{2}{\nu} \sqrt{\frac{\log(2m/p_3)}{2n}}$

write

$$V = \sup_{\pi \in \Pi, \phi \in \Phi} (\mathbb{E}_n - \mathbb{E})(\pi(T|X)(1 - \phi(X)) - \pi_c(T|X))WY \quad (26)$$

Since it has bounded difference of  $\frac{B}{n\nu}$ , McDiarmid' inequality indicates with probability  $1 - p_4$ ,

$$V - \mathbb{E}V \leq \frac{B}{\nu} \sqrt{\frac{\log \frac{1}{p_4}}{2n}} \quad (27)$$

By the symmetrization argument,

$$\mathbb{E}V \leq 2\mathbb{E} \sup_{\pi \in \Pi, \phi \in \Phi} \frac{1}{n} \sum_i \epsilon_i (\pi(T_i|X_i)(1 - \phi(X_i)) - \pi_c(T_i|X_i)) W_i Y_i \quad (28)$$

By Rademacher comparison theorem / contraction principle ([51], Thm 4.12),

$$\mathbb{E}V \leq 2\frac{B}{\nu} \mathbb{E}\mathfrak{R}_n(\Pi) \quad (29)$$

Finally, with probability  $1 - p_5$ , since  $\mathfrak{R}_n(\Pi)$  has bounded differences with  $\frac{2}{n}$ , by McDiarmid's inequality we have

$$\mathbb{E}\mathfrak{R}_n(\Pi) - \mathfrak{R}_n(\Pi) \leq \sqrt{\frac{2}{n} \log \frac{1}{p_5}}. \quad (30)$$

Similarly, with probability  $1 - p_6$ , we have

$$\mathbb{E}\mathfrak{R}_n(\Phi) - \mathfrak{R}_n(\Phi) \leq \sqrt{\frac{2}{n} \log \frac{1}{p_6}}. \quad (31)$$

Let  $p_1 = p_2 = p_3 = p_4 = p_5 = p_6 = \frac{\delta}{6}$ ,

$$\sup_{\pi \in \Pi, \phi \in \Phi} R(\pi, \phi, \pi_c) - \hat{R}(\pi, \phi, \pi_c, \mathcal{W}^*) \quad (32)$$

$$\leq (3B + 3\bar{c} + \frac{1}{\nu} + \frac{2B}{\nu^2} + \frac{3B}{\nu}) \sqrt{\frac{2 \log \frac{\max(6, 8m)}{\delta}}{n}} + 2\frac{B}{\nu} \mathfrak{R}_n(\Pi) + 2(B + \bar{c}) \mathfrak{R}_n(\Phi) \quad (33)$$

$$\leq (3B + 3\bar{c} + \frac{5B + 1}{\nu^2}) \sqrt{\frac{2 \log \frac{8m}{\delta}}{n}} + 2\frac{B}{\nu} \mathfrak{R}_n(\Pi) + 2(B + \bar{c}) \mathfrak{R}_n(\Phi) \quad (34)$$

Since we have the well-specification assumption, thus  $\hat{R}(\pi, \phi, \pi_c, \mathcal{W}^*) \leq \hat{R}(\pi, \phi, \pi_c, \mathcal{W}_n^\Gamma)$ , which completes the proof.  $\square$

Proof of Theorem 2.

*Proof.* We prove the claim by contradiction. Suppose  $r_1 \leq \dots \leq r_n$ , and suppose the optima  $W^*$  has  $W_i^* = b_i$ ,  $W_j^* = a_j$  with  $i < j$ . It means

$$\begin{aligned} 0 &< \frac{\partial}{\partial W_i} \frac{\sum_{i=1}^n r_i W_i}{\sum_{i=1}^n W_i} \\ &= \sum_{k \neq i, j} (r_i - r_k) W_k + (r_i - r_j) W_j \\ &\leq \sum_{k \neq i, j} (r_j - r_k) W_k + (r_j - r_i) W_i \\ &= \frac{\partial}{\partial W_j} \frac{\sum_{i=1}^n r_i W_i}{\sum_{i=1}^n W_i}, \end{aligned}$$

where the inequality is because  $r_i \leq r_j$ ,  $(r_i - r_j)W_j \leq 0 \leq (r_j - r_i)W_i$ . The partial derivative means the objective increases with  $W_j$ , which contradicts the assumption that the optimal  $W_j^*$  equals its minimal value  $a_j$ . Therefore, for the optimal  $W^*$ , there exists  $k \in \{1, \dots, n\}$  such that  $W_i^* = b_i$  for  $i \geq k$  and  $W_i^* = a_i$  for  $i < k$ .  $\square$

## B Baselines

Here we include more details about the baselines we used in the experiments.

**Human Only (Human):** Human only solely queries human-decision-makers randomly to output final decisions and each human decision maker will incur a cost of  $C(X_i)$ .

**Algorithm Only (AO):** uses the inverse propensity score weighting method to train a policy. AO solves the following optimization problem:

$$\min_{\pi \in \Pi} \frac{1}{N} \sum_{i=1}^N \frac{\pi(T_i|X_i)}{\hat{\pi}_0(T_i|X_i)} Y_i, \quad (35)$$

which can be efficiently solved by gradient descent for differentiable policy classes.

**Confounding-Robust Algorithm Only (ConfAO)** trains a confounding-robust policy [47] to determine the final decisions. ConfAO solves a constraint optimization of the AO baseline with the marginal sensitivity model constraint on the nominal propensity scores. More specifically, it optimizes the following objective:

$$\min_{\pi \in \Pi} \max_{\pi_0} \frac{1}{N} \sum_{i=1}^N \frac{\pi(T_i|X_i)}{\pi_0(T_i|X_i, Y_i)} Y_i \quad (36)$$

$$s.t. \quad \Gamma_i^{-1} \leq \frac{(1 - \tilde{\pi}_0(T_i|X_i)\pi_0(T_i|X_i, Y_i))}{\tilde{\pi}_0(T_i|X_i)(1 - \pi_0(T_i|X_i, Y_i))} \leq \Gamma_i. \quad (37)$$

Similar to our method, it also requires a pre-specified  $\Gamma$  to ensure robustness against unobserved confounding, while not considering the possibility for human to make future decisions.

**Human-AI team (HAI)** uses the deferral collaboration method proposed in [4] to train a router and policy jointly assuming unconfoundedness. It optimizes the policy and router jointly using the objective:

$$\min_{\phi \in \Phi, \pi \in \Pi} \sum_{i=1}^N \phi(X_i)(Y_i + C(X_i)) + \frac{(1 - \phi(X_i))\pi(T_i|X_i)}{\hat{\pi}_0(T_i|X_i)} Y_i. \quad (38)$$

## C Additional Details about Experiments

In this section, we provide more details about the datasets we used. We use the logistic policies for the policy and router model classes.

**Financial Lending.** For HELOC dataset, we use the following features in the experiments: number of months that have elapsed since first trade, number of months that have elapsed since last opened trade, average months in file, number of satisfactory trades, number of trades which are more than 60 past due, number of trades which are more than 90 past due, percent of trades, that were not delinquent, number of months that have elapsed since last delinquent trade, the longest delinquency period in last 12 months, the longest delinquency period, total number of trades, number of trades opened in last 12 months, percent of installments trades, months since last inquiry (excluding last 7 days), number of inquiries in last 6 months, number of inquiries in last 6 months (excluding last 7 days), revolving balance divided by credit limit, installment balance divided by original loan amount, number of revolving trades with balance, number of installment trades with balance, number of trades with high utilization ratio (credit utilization ratio - the amount of a credit card balance compared to the credit limit), and the percent of trades with balance. The outcome of the dataset is a binary outcome indicating whether the applicant was 90 days past due since the account was opened over 24 months. HELOC dataset has 10459 observations, 5000 of which has ‘good’ credit and ‘5459’ has bad credit. We use 10% of the data to generate the observational data and the rest as test data with 10 random partitions.

**Acute Stroke Treatment.** For the International Stroke Trial data, we use the following features: age, sex, conscious state, systolic blood pressure, pulmonary embolism, deep vein thrombosis, infarct visible on CT, face deficit, arm/hand deficit, leg/foot deficit, dysphasia hemianopia, visuospatial disorder, brainstem/cerebellar signs, other deficit and stroke type. Our scalarized composite score is:

$$Y = 2\mathbb{I}[\text{death at discharge}] + \mathbb{I}[\text{recurrent stroke}] + 0.5\mathbb{I}[\text{pulmonary embolism or intracranial bleeding}] + 0.5\mathbb{I}[\text{other side effects}] - 2\mathbb{I}[\text{full recovery}] - \mathbb{I}[\text{discharge}]$$

For categorical variables, we use one-hot encodings as features, which results in 42 features

in total. The dataset has 19435 patients with acute ischaemic stroke, since we only focus on patients who are assigned aspirin with median, high, or none heparin dose, it results in 2430 samples in the treated group (more aggressive treatment) and 4858 samples in the control treatment (only aspirin). We randomly split data into 50%/50% train-test split with 10 runs.